

## Epoxidized pine oil-siloxane: Crosslinking kinetic study and thermomechanical properties

Mohamed A. Abdelwahab,<sup>1\*</sup> Manjusri Misra,<sup>1,2</sup> Amar K. Mohanty<sup>1,2</sup>

<sup>1</sup>Bioproducts Discovery and Development Centre, University of Guelph, Guelph, Ontario N1G 2W1, Canada

<sup>2</sup>School of Engineering, Thornbrough Building, University of Guelph, Guelph, Ontario N1G 2W1, Canada

\*On leave from Department of Chemistry, Tanta University, Tanta 31527, Egypt.

Correspondence to: M. Misra (E-mail: mmisra@uoguelph.ca) and A. K. Mohanty (E-mail: mohanty@uoguelph.ca)

**ABSTRACT:** In this study, a novel approach to toughen biobased epoxy polymer with different types of siloxanes was explored. Three different modified siloxanes, e.g., amine-terminated polydimethyl siloxane (PDMS-amine), glycidyl-terminated polydimethyl siloxane (PDMS-glycidyl), and glycidyl-terminated polyhedral oligomeric silsesquioxane (POSS-glycidyl) were used as toughening agents. The curing and kinetics of bioepoxy was investigated by differential scanning calorimetry and Fourier transform infrared spectroscopy. The mechanical, thermal, and morphological properties of the cured materials were investigated. Rheological characterization revealed that the inclusion of POSS-glycidyl slightly increased the complex viscosity compared to the neat resin. The morphology of the cured bioresin was characterized by transmission electron microscopy and scanning electron microscopy. The inclusion of POSS-glycidyl to bioepoxy resin resulted in a good homogeneity within the blends. The inclusion of PDMS-amine or PDMS-glycidyl was shown to have no effect on tensile and flexural properties of the bioresins, but led to a deterioration in the impact strength. However, the inclusion of POSS-glycidyl enhanced the impact strength and elongation at break of the bioresins. Dynamic mechanical analysis showed that the siloxane modified epoxy decreased the storage modulus of the bioresins. The thermal properties, such as decomposition temperature, coefficient of linear thermal expansion, and heat deflection temperature were improved by inclusion of POSS-glycidyl. © 2015 Wiley Periodicals, Inc. *J. Appl. Polym. Sci.* **2015**, *132*, 42451.

**KEYWORDS:** biopolymers and renewable polymers; blends; crosslinking; mechanical properties; thermosets

Received 18 September 2014; accepted 23 April 2015

DOI: 10.1002/app.42451

### INTRODUCTION

In recent years, renewable raw materials for the production of thermoplastic and thermoset polymers have attracted a great deal of attention from both the academic and industrial communities to substitute petroleum based polymers.<sup>1</sup> Epoxy resins are one of the key commercial thermoset polymers owing to their superior chemical resistance, mechanical properties and good processability. Therefore, epoxy resins are useful in different applications, such as adhesives, coatings, insulating materials, electronics and structural composites. Nowadays, epoxy resins are used in automobile assembly, aircrafts, aerospace, and wind turbine blades.<sup>1</sup> However, epoxy resin has some disadvantages such as high cost, brittleness, low elongation at break, and impact strength as well as a poor resistance to crack growth.<sup>2</sup> Many efforts have been made to overcome the drawbacks of epoxy resins by the addition of inorganic fillers,<sup>3,4</sup> use of thermoplastic particles,<sup>5</sup> or the addition of a second rubbery phase.<sup>5–7</sup>

Recently, a number of biobased epoxy resins made from plant oils have been reported.<sup>8–12</sup> Plant oils, which contain long chain fatty acids, are available widely from various natural resources. Soybean oil and linseed oil were found to be the most common oils used today due to their availability and low cost.<sup>13</sup> Epoxidized soybean oil (ESO), which is derived from soybean oil, has been used in many applications, such as plasticizers for plastics, stabilizers, or as a toughening agent for petroleum-based epoxy resins.<sup>14</sup> ESO shows superior potential as a renewable and an inexpensive material for some industrial applications.<sup>15</sup>

ESO can be used to enhance the toughness of epoxy resin and its addition to epoxy helps also to decrease the cost of the final product. Ratna<sup>16</sup> reported a blend of ESO with an epoxy resin. Phase separation was found in the blend resulting in higher impact strength. Miyagawa *et al.*<sup>9</sup> prepared a biobased epoxy blend from diglycidyl ether of bisphenol F (DGEBF) and ESO with an anhydride curing agent which showed enhancement in the impact strength and fracture toughness due to the phase

separation. Gupta *et al.*<sup>10</sup> studied the effect of addition ESO into a diglycidyl ether of bisphenol A (DGEBA) based epoxy resin with different weight ratios. It was reported that the lower the concentration of DGEBA based epoxy resin, the better the impact properties. Nowadays, biobased epoxy resins with different amount of epoxy groups are commercially available and can be used in different applications.<sup>17,18</sup>

However, biobased epoxy has some disadvantages such as low mechanical performance and heat deflection temperature compared to commercial epoxy resin. Fillers are required to overcome some of these hurdles and to fulfill certain industrial requirements.<sup>11</sup> Polydimethyl siloxane (PDMS) is a type of silicone rubber that possesses superior properties, such as good chemical and thermal resistance, high elasticity, and good hydrophobic properties.<sup>19–21</sup> The addition of PDMS into the epoxy system is typically a challenge due to the immiscibility between polar epoxy resin and nonpolar PDMS polymer before and after curing.<sup>22–24</sup> An alternative way to enhance the compatibility between PDMS and epoxy resin is to functionalize PDMS with amine or hydroxyl group to enhance its miscibility with epoxy. It is expected that hydroxyl or amine terminated PDMS can bond to epoxy resin leading to an enhancement in some mechanical properties due to incorporation of a rubbery segment in the network. Gong *et al.*<sup>22</sup> were able to toughen epoxy resin with a block copolymer consisting of amine-terminated PDMS and a hydroxy-terminated-oligo (hydroxyether of bisphenol A). In another study, epoxy resin was modified using hydroxyl-terminated PDMS in the presence of dibutyltindilaurate as a catalyst and  $\gamma$ -aminopropyltriethoxysilane as a crosslinking agent.<sup>20</sup> They found that a siliconized epoxy system has a higher thermal stability and a heterogeneous morphology compared to a regular epoxy system.

Another approach to toughen epoxy resin is to introduce a hybrid inorganic–organic composition of polyhedral oligomeric silsesquioxanes (POSS), a nanosized cage structure, into the polymeric chain via covalent bonding. POSS possesses a desirable balance of toughness and stiffness as well as a good thermal stability.<sup>25–27</sup> The addition of functionalized POSS into the epoxy resin can enhance the mechanical properties.<sup>28–32</sup> In this regard, glycidyl-terminated POSS (POSS-glycidyl) can be used as a toughener for epoxy system to enhance the toughening behavior of epoxy. Kim *et al.*<sup>33</sup> displayed the thermo-mechanical and morphological properties of POSS-epoxy based on octaglycidyl-epoxy-polyhedral-oligosilsesquioxane (OG-POSS) using different ratios of a hardener (4,4'-diaminodiphenyl sulfone (DDS)). They found that by increasing the amount of DDS, the glass transition temperature ( $T_g$ ) increased and the structure become more homogeneous. Li *et al.*<sup>34</sup> showed the increasing POSS concentration in POSS-glycidyl-modified epoxy resin enhanced the thermal stress coefficient.

The aim of this work is to develop a novel siliconized bioepoxy using different functionalized siloxanes, such as amine-terminated PDMS, glycidyl-terminated PDMS, and POSS-glycidyl in the bioepoxy resin. The kinetics, mechanical, thermal, and the morphological properties of biobased resin modified with different siloxanes were then characterized and analyzed.

## EXPERIMENTAL

### Materials

Biobased epoxy resin (bioepoxy) was a Super sap INF that was supplied by Entropy Resin, composed of epoxy and hardener in liquid form. The bioepoxy contain biobased renewable materials extracted as a coproduct from waste streams of industrial processes, such as biofuel and wood pulp production. The epoxy is a mixture of epoxidized pine oils, bisphenol A/F type, and benzyl alcohol. The hardener is a mixture of cyclohexanemethanamine, 5-amino-1,3,3-trimethyl isophoronediamine (20–50%), polyoxy propylene diamine (30–60%), *tris*-2,4,6-(dimethylaminomethyl)phenol (10–20%), *bis*(dimethyl-amino-methyl)phenol (<10%), benzyl alcohol (<10%), piperazine (<10%), and aminoethyl piperazine (<5%). Bioepoxy is claimed to have up to 19% biobased content. The recommended bioepoxy resin to hardener ratio was 100:33 by weight. Polydimethyl siloxane-*bis*(3-amino propyl) terminated (PDMS-amine) with average molecular weight ( $M_n$ ) of 2500 and polydimethyl siloxane-diglycidyl ether terminated (PDMS-glycidyl) with average  $M_n$  of 800 were purchased from Sigma-Aldrich. The POSS-glycidyl used is a polyepoxyglycidyl silsesquioxane cage mixture (EP0409 glycidyl POSS cage mixture, from Hybrid Plastics). The POSS-glycidyl has an epoxide equivalent weight of 167 g/equiv. The chemical structures of all modified siloxanes are shown in Scheme 1.

### Sample Preparation

Biobased formulation were prepared by mixing bioepoxy with 5 wt % of PDMS-amine, PDMS-epoxy, or POSS-glycidyl. All compositions were mixed at room temperature until the mixture was homogeneous. Then, the hardener was added to all systems. The mixtures were degassed at room temperature to remove bubbles and poured into the prepared mold for complete curing. The bioresins were cured at room temperature for 24 h and then at 100°C for 1 h and postcured at 150°C for 1 h.

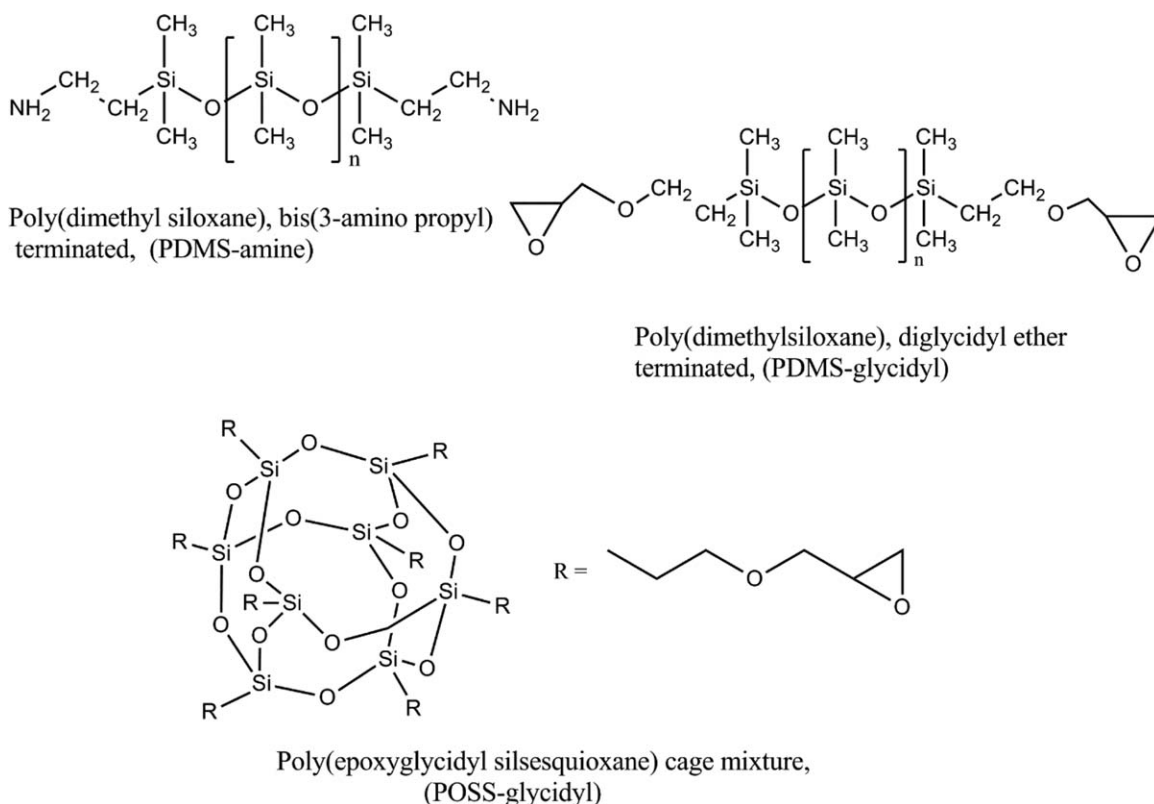
### Characterization

The attenuated total reflection infrared (ATR-IR) was conducted through the use of a Nicolet™ 6700 FTIR spectrometer (Thermo Scientific) with transmittance range of 400–4000  $\text{cm}^{-1}$  and resolution of 4  $\text{cm}^{-1}$  with 64 scans per sample.

Instron 3382 (universal testing machine) was used to achieve flexural and tensile properties in accordance with ASTM D790 and D638 standards, at speed of 14 and 5 mm/min, respectively. Impact strength was performed on a TMI 43-02 impact testing device in accordance with ASTM D256 using 5 ft-lb pendulum. The notched depths of 2 mm were conducted using a TMI notching cutter. All samples (5 samples) were kept at room temperature for 48 h before performing the tests.

Thermal behavior and kinetics of the bioepoxy and modified bioepoxy were performed by differential scanning calorimetry (DSC) (TA Instrument DSC Q200) under nitrogen atmosphere with flow rate of 50 mL/min at rate of 10°C/min. In dynamic tests, the samples (5–8 mg) were heated from –50 to 300°C at various heating rates (2, 5, 7, 10, and 20°C/min).

Thermal stability of the bioresins was tested using TGA Q500 (TA Instruments, USA) under nitrogen gas flow rate of 60 mL/min and heating rate 10°C/min.



**Scheme 1.** Chemical structure of PDMS-amine, PDMS-epoxy, and glycidyl-POSS.

The static heat-resistant temperature ( $T_s$ ) is calculated by the equation:

$$T_s = 0.49 [T_5 + 0.6 (T_{30} - T_5)] \quad (1)$$

where  $T_5$ ,  $T_{30}$  are the weight loss at 5 and 30%, respectively

Dynamic mechanical analysis (DMA) was achieved using a DMA (TA Instruments Q800). A clamp was used at oscillating amplitude of 15 mm and frequency of 1 Hz. The bioresins were scanned from  $-70$  to  $110^\circ\text{C}$  at a rate of  $3^\circ\text{C}/\text{min}$ .

Heat deflection temperature (HDT) of the bioepoxy resins was measured using DMA in three point bending mode under the applied load of 0.455 MPa. Samples were heated from room temperature to desired temperature at a ramp rate of  $2^\circ\text{C}/\text{min}^{-1}$ . Temperature corresponding to a deflection of 0.25 mm was recorded as the HDT of the sample.

The CLTE (coefficient of linear thermal expansion) of the neat bioepoxy and modified bioepoxy were measured by an expansion probe using a TMA (TA Instruments 2940). Testing was performed at a heating rate of  $5^\circ\text{C}/\text{min}$  with force of 0.1N and temperature range of 35 to  $160^\circ\text{C}$ . The CLTE was calculated from the straight line in the range of  $100$ – $150^\circ\text{C}$ .

The viscosity of bioepoxy and modified bioepoxy were tested on a rheometer Anton Paar MCR302 (Graz, Austria) using Ball measuring system (BMS). The experiment was done at room temperature with fixed strain (1%) and fixed angular frequency (1 rad/s).

Morphological examination of the fractured impact surfaces of the bioresins was performed using a Phenom ProX w/Prosuite

high resolution desktop scanning electron microscope (SEM), from nanoScience Instruments, USA at voltage of 20 kV.

The transmission electron microscopy (TEM) was taken through microscope FEI Tecnai G2. Around 80 nm thick section were cut with ultramicrotome Leica Ultracut UCT using diamond knife (Leica Microsystems).

Density was measured using electronic densimeter (Alfa Mirage MD-300 S) according to Archimedes principle.

## RESULTS AND DISCUSSION

### Curing Behavior and Curing Activity

The dynamic (nonisothermal) curing of neat and siloxane-blended bioepoxies were studied by DSC. Figure 1 displays the DSC of neat bioepoxy at different heating rates between 2 and  $20^\circ\text{C}/\text{min}$ . DSC of neat bioepoxy resin exhibits a single broad exothermic peak. This is due to reaction between epoxide groups of bioepoxy with the amino group of the hardener. The reaction starts at around  $34^\circ\text{C}$  and the temperature of maximum rate occurs between 75 and  $120^\circ\text{C}$  depending on the heating rate. By increasing the heating rate, the magnitude of the exothermic increases as well. The maximum temperature exothermic peak shifts to a higher temperature by increasing the heating rate. In Figure 2, the initial ( $T_{\text{initial}}$ ), maximum ( $T_{\text{maximum}}$ ), and final temperature ( $T_{\text{final}}$ ) were collected and plotted versus heating rate. The linear fit of  $T_{\text{initial}}$  and  $T_{\text{final}}$  at heating rate equal to zero is used as a reference for curing temperature and postcuring temperature, respectively.<sup>35</sup> In order to confirm the completion of curing, temperature from 0 to  $20^\circ\text{C}$  higher than  $T_{\text{initial}}$  and  $T_{\text{final}}$  are used as the cure and postcure

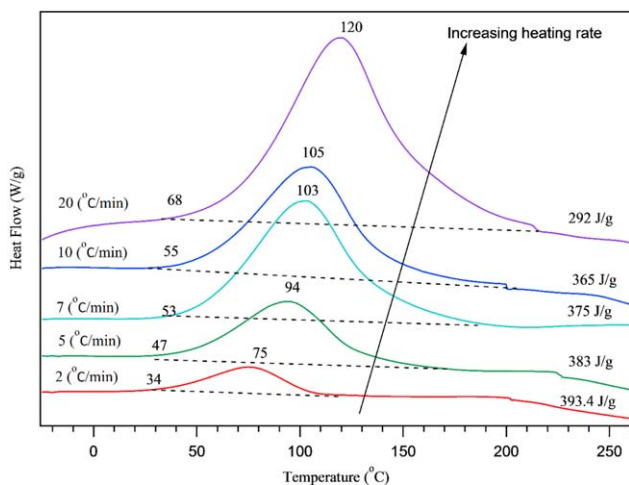


**Figure 1.** Nonisothermal DSC cure behavior of neat bioepoxy resin at different heating rates. [Color figure can be viewed in the online issue, which is available at [wileyonlinelibrary.com](http://wileyonlinelibrary.com).]

temperatures. From Figure 2, the  $T_{\text{initial}}$  and  $T_{\text{final}}$  values are 35 and 110°C, respectively. The neat bioepoxy was cured at room temperature overnight then cured at 100°C for 1 h then post-cured at 150°C for 1 h.

The activation energy of neat bioepoxy was studied using two approaches: the first one is Kissinger's approach:<sup>36</sup>

$$\ln\left(\frac{\beta}{T_p^2}\right) = \ln\left(\frac{AR}{E_a}\right) - \left(\frac{E_a}{RT_p}\right), \quad (2)$$

where  $\beta$  is the constant heating rate,  $T_p^2$  is the square of maximum temperature of the exothermic peak,  $A$  is the pre-exponential factor, and  $R$  is the gas constant ( $R=8.314$  kJ/molK). The values of activation energy ( $E_a$ ) and pre-exponential factor ( $A$ ) can be obtained by plotting  $\ln\left(\frac{\beta}{T_p^2}\right)$  versus  $1/T_p$  and calculating the slope of the linear fit.

The second one is Flynn-Wall-Ozawa approach where the degree of conversion is constant at different heating:<sup>37</sup>

$$\log\beta = \frac{-0.4567E_a}{RT_p} + C, \quad (3)$$

where  $\beta$  is the constant heating rate,  $T_p$  is the maximum temperature of exothermic peak,  $R$  is the gas constant, and  $C$  is a constant. The activation energy and  $C$  can be obtained from the slope and the intercept, respectively, by plotting  $\log\beta$  versus  $1/T_p$ . We selected these two approaches since they do not need any information of the reaction mechanism to calculate the kinetics. Figure 3(i,ii) shows the plots of  $\ln\left(\frac{\beta}{T_p^2}\right)$  versus  $1/T_p$  based on Kissinger's approach (equation (2)) and  $\log\beta$  versus  $1/T_p$  based on the Flynn-Wall-Ozawa equation (3) for neat bioepoxy. The  $E_a$  can be calculated from both equations and was found to be 55.419 and 52.14 kJ/mol, based on eqs. (2) and (3), respectively.

The kinetics of bioepoxy with different siloxanes was studied using Flynn-Wall-Ozawa and Kissinger equations [Figure 3(iii)]. It was found that the activation energy of the blended bioepoxy had a higher value compared to the neat bioepoxy as shown in Figure 3(iii). This could be due to the phase separation of

PDMS amine or PDMS glycidyl that could hinder the reaction between the epoxy group and the curing agent. Thomas *et al.*<sup>2</sup> reported the activation energy increased with the introduction of acrylonitrile liquid rubber (CTBN) and carboxyl-terminated copolymer of butadiene to DGEBA. The author explained that the increase in the activation energy is attributed to the phase separation between the liquid rubber and the bioepoxy matrix. However, the frame network formed by POSS-POSS interaction led to an increase of the pseudocuring density which increased the activation energy of bioepoxy modified with POSS-glycidyl. It can be observed that the activation energy calculated by Flynn-Wall-Ozawa method is slightly higher than the activation energy obtained by Kissinger method for all resins as observed in other traditional epoxy systems.<sup>38</sup>

### Curing Study of the Bioepoxy Modified with Siloxane by FTIR

The FTIR spectra of neat bioepoxy, neat hardener and bioresin after different crosslinking conditions are shown in Figure 4, and characteristic bands are tabulated in Table I. The peak attributed to the crosslinking reaction of epoxy group with hardener (860 and 915  $\text{cm}^{-1}$ ) gradually decreased with increasing temperature. Also, the peak at 771  $\text{cm}^{-1}$ , corresponding to the amino group, decreased.

To confirm complete curing of modified bioepoxy samples, FTIR spectra were taken and shown in Figure 5. All bioresins showed the disappearance of epoxy band at 914  $\text{cm}^{-1}$ . The reaction between bioepoxy and PDMS terminated amine and glycidyl was confirmed by the presence of strong absorption bands around 1230, 1100–1000, and 798  $\text{cm}^{-1}$  corresponding to  $\text{CH}_3$  symmetric bending, Si–O–Si stretch and Si–C stretch, respectively.<sup>39</sup> Moreover, the absorption band at 1100  $\text{cm}^{-1}$  confirms the existence of siloxane Si–O–Si vibration of POSS-glycidyl in the modified bioepoxy.

### Effect of Additives on the Viscosity

In order to investigate the effects of different siloxanes on the gelation process, the pot-life time of the bioresins must be measured through reaction kinetics. The experiment was performed at room temperature with fixed strain (1%) and fixed

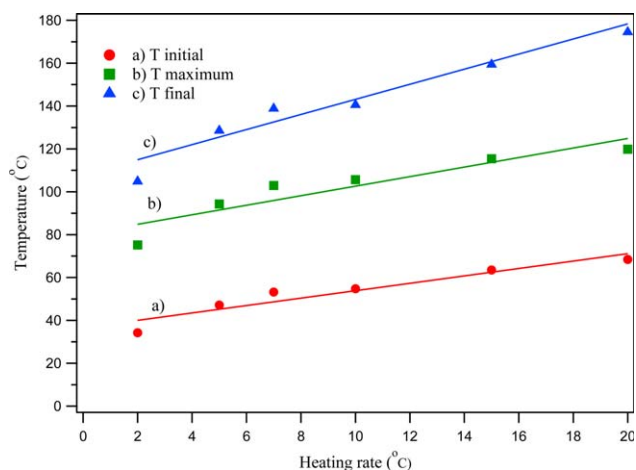


**Figure 2.**  $T_{\text{initial}}$ ,  $T_{\text{maximum}}$ , and  $T_{\text{final}}$  of bioepoxy resin at different heating rates. [Color figure can be viewed in the online issue, which is available at [wileyonlinelibrary.com](http://wileyonlinelibrary.com).]



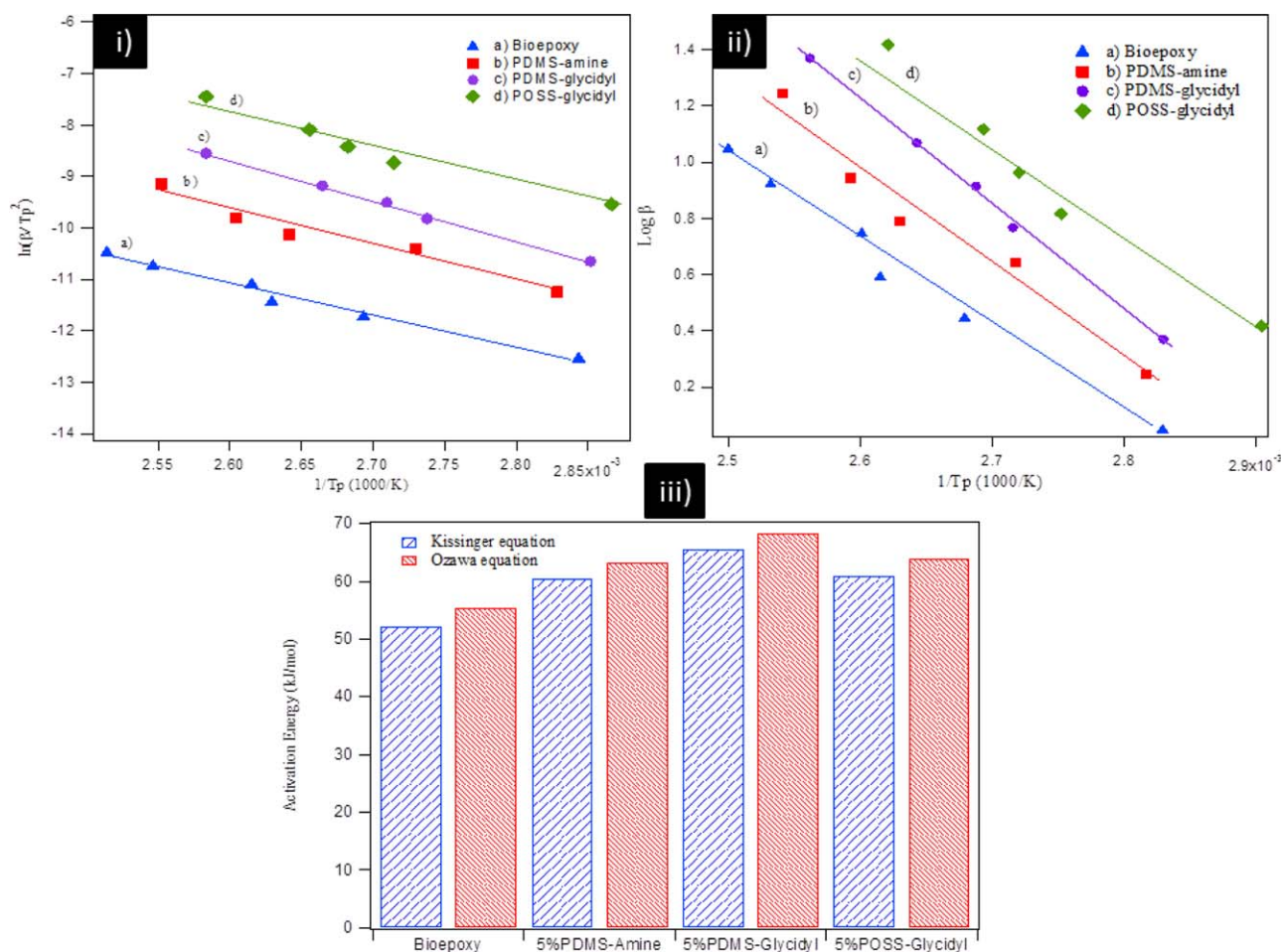


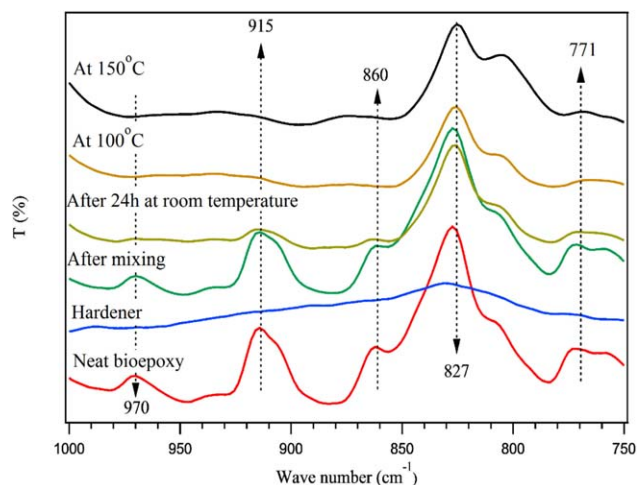
**Figure 3.** Plot for the determination of activation energies based on Kissinger method (i) and Flynn-Wall-Ozawa method (ii) for neat bioepoxy and bioepoxy modified by siloxanes, respectively. (iii) Activation energy of neat bioepoxy and bioepoxy modified by siloxanes obtained by Kissinger and Flynn-Wall-Ozawa method. [Color figure can be viewed in the online issue, which is available at [wileyonlinelibrary.com](http://wileyonlinelibrary.com).]

angular frequency (1 rad/s). Figure 6 shows the graphs of the logarithm of complex viscosity versus time for neat and modified bioepoxy. Neat bioepoxy showed an improvement in the viscosity with respect to time. This is due to the reaction between the amino group present in the hardener and the epoxy group present in the bioepoxy which leads to crosslinking. Moreover, all three modified siloxane bioepoxy showed an enhancement in the viscosity similar to the behavior of the neat resin. However, at the room temperature (25°C), the inclusion of POSS-glycidyl increased the complex viscosity from around 2 to 2.25 Pa S compared to neat bioepoxy, which may be due to excess of glycidyl group present in the POSS-glycidyl which accelerate the epoxy-network formation.<sup>40</sup> The time necessary for the formation of the POSS-glycidyl network is higher than that of PDMS-amine and PDMS-glycidyl.

### Morphology of Bioresins

The SEM micrographs of neat bioepoxy resin and siloxanes modified resin are displayed in Figure 7 (i). Neat bioepoxy shows an irregular-layer break morphology [Figure 7(i) a]. Bioepoxy with PDMS-glycidyl or amine-terminated displays domains with white and dark particles as shown in Figure 7(i)

b and (i) c. These domains are preferentially dispersed as sphere shape in the continuous bioepoxy resin. The approximate diameters of these domains were in the sort of around 10  $\mu\text{m}$

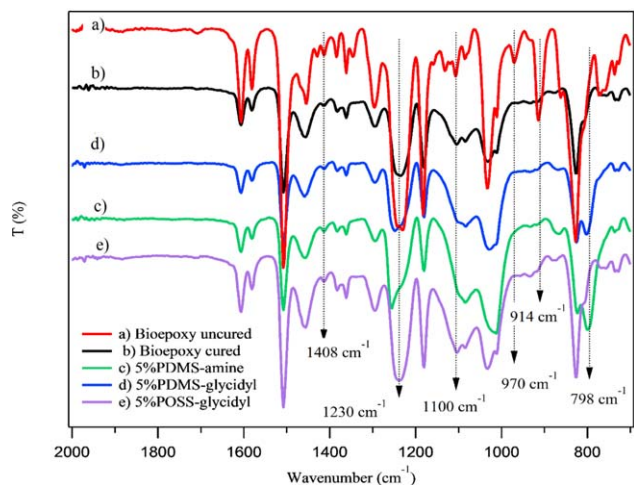
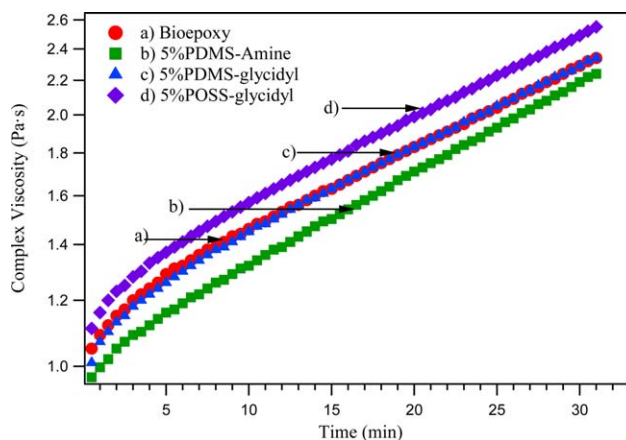


**Figure 4.** FTIR spectra of neat bioepoxy, hardener, after mixing, at room temperature, at 100 and 150°C. [Color figure can be viewed in the online issue, which is available at [wileyonlinelibrary.com](http://wileyonlinelibrary.com).]

**Table I.** Attribution of the FTIR Absorption Bands of Bioepoxy and Hardener

Wavenumber (cm <sup>-1</sup> )	Assignments
Bioepoxy resin	
771	Rocking CH <sub>2</sub>
827	Stretching C—O—C of oxirane group and out of plane deformation of the aromatic CH
860	Stretching C—O—C of oxirane group
915	Characteristic vibration band (symmetric) of the epoxy ring
1034	Stretching C—O—C of ethers
1182	Stretching —C—C—O—C
1362	Deformation CH <sub>3</sub> of C—(CH <sub>3</sub> ) <sub>2</sub>
1454	Deformation C—H of CH <sub>2</sub> and CH <sub>3</sub>
1508	Stretching C—C of aromatic
1606	Stretching C=C of aromatic rings
2800–2990	Stretching C—H of CH <sub>2</sub> and CH aromatic and aliphatic
3057	Stretching of C—H of the oxirane ring
3521	O—H stretching
Hardener amine	
1456	Secondary N—H deformation
1597	Secondary N—H deformation
2840–2950	Stretching of C—H of the oxirane ring
3360, 3280, 3180	Primary amines, doublet (reflecting the symmetric and antisymmetric stretching modes)

in the resins. The dispersed phase surface is clear and flat borders exist which suggest the poor compatibility between the phases (Scheme 2). However in Figure 7(i) d, the surface of bioepoxy with 5%POSS-glycidyl had a smoother break with no evi-

**Figure 5.** FTIR spectra of uncured and cured neat bioepoxy and cured bioepoxy modified by different siloxanes. [Color figure can be viewed in the online issue, which is available at wileyonlinelibrary.com.]**Figure 6.** Complex viscosity versus time of neat bioepoxy and bioepoxy modified by different siloxanes. [Color figure can be viewed in the online issue, which is available at wileyonlinelibrary.com.]

dence of phase separation. Ni *et al.*<sup>41</sup> showed that the inclusion of POSS—NH<sub>2</sub> modified with *n*-butyl glycidyl ether displayed rough section surface with epoxy resin. Here, the POSS-glycidyl uniformly dispersed in the bioepoxy resin which represents improvement in the compatibility between the matrix and the modifier (Scheme 2).

The dispersion of POSS-glycidyl in bioepoxy was further confirmed by TEM analysis. Figure 7(ii) shows the TEM micrograph of bioepoxy/5%POSS-glycidyl in different sections. It can be seen that the POSS-glycidyl (dark areas) are well dispersed in the bioepoxy matrix [Figure 7(ii) a]. The spherical domain size in the bioblend is approximately 20–60 nm. However, a number of dark spots and agglomeration appear in Figure 7(ii) b with a size of approximately 60–100 nm. The strong POSS–POSS interaction leads to aggregates within bioepoxy matrix. Strachota *et al.*<sup>42</sup> assumed some nanoaggregates by the incorporation of POSS into network of DGEBA. This is due to the steric hindrance in the POSS-glycidyl which provides inhomogeneous distribution of POSS-glycidyl within matrix.

### Mechanical Properties

The mechanical characteristics of the bioepoxy resin modified with siloxanes are shown in Figures 8 and 9. In general, neat bioepoxy resin has low impact strength and elongation at break with high tensile and flexural properties. The tensile modulus and strength of neat bioepoxy was found to be 3.28 GPa and 68.8 MPa, respectively (Figure 8). The incorporation of PDMS-amine or PDMS-epoxy showed a slight decrease in the tensile and flexural strength compared to the bioepoxy resin. These results indicate that the incorporation of elastomeric PDMS segments results in a reduction in the crosslinking density, which decreases the tensile properties.<sup>43</sup> Moreover, there is no compatibility between the polar bioepoxy and nonpolar functional PDMS, leading to phase separation at the interface as indicated by the SEM analysis. However, the incorporation of 5%POSS-glycidyl showed a 7% increase in the tensile strength. This is due to the reaction between the glycidyl groups of POSS with the bioepoxy system, which increases the crosslinked density of the network and decreases the free volume of epoxy backbone.<sup>44</sup>



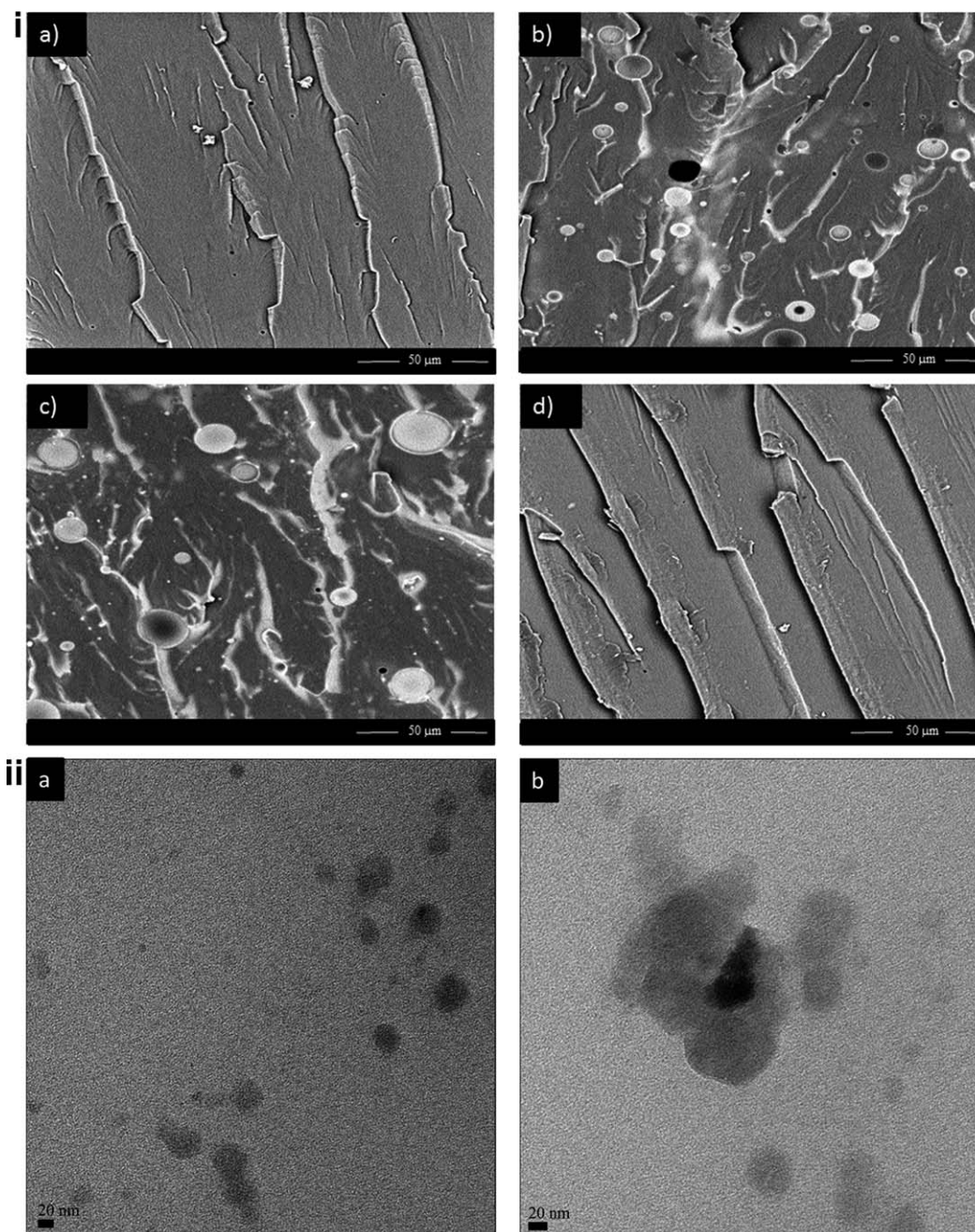


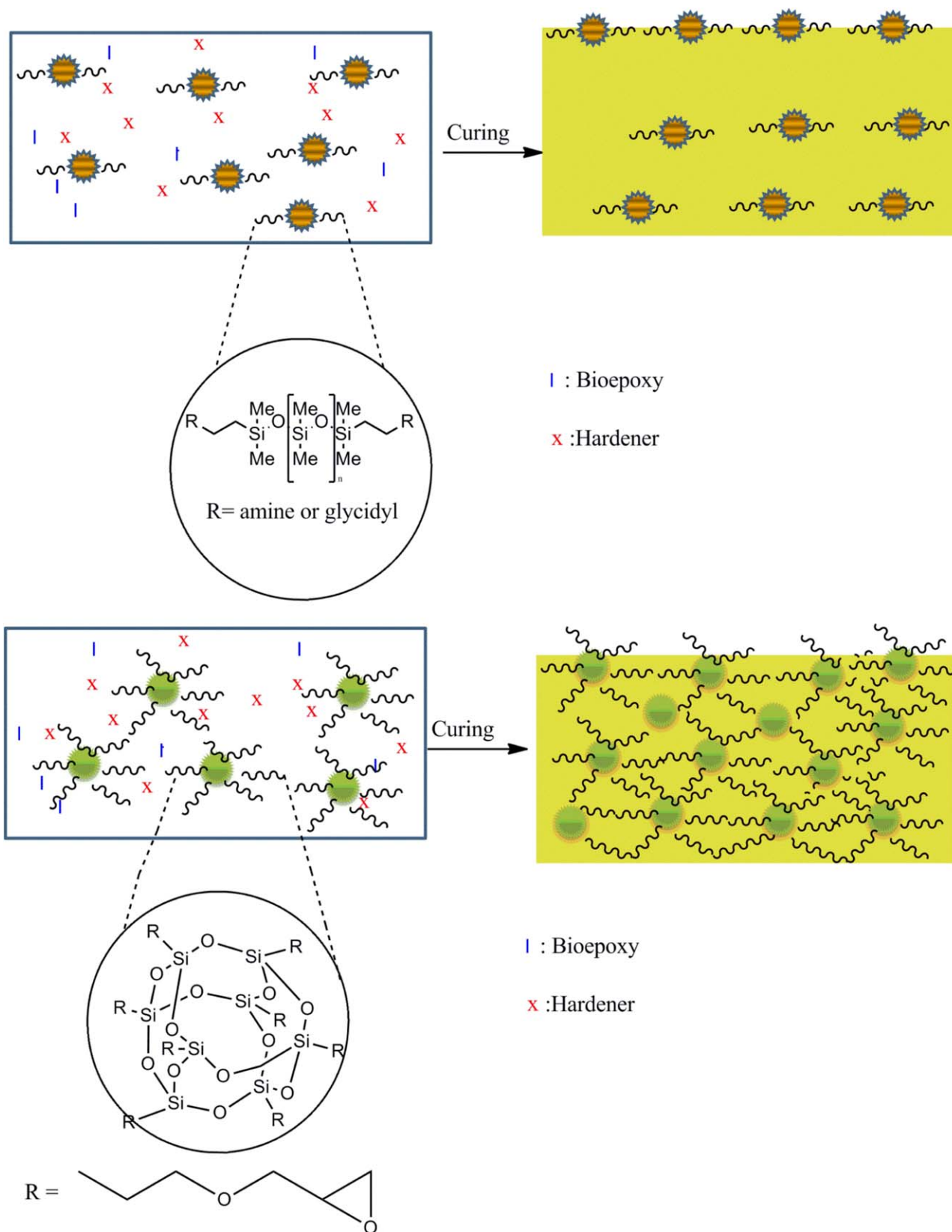
**Figure 7.** (i) Scanning electron microscope images of (a) neat bioepoxy (1500 $\times$ ), (b) bioepoxy/5%PDMS-amine, (c) bioepoxy/5%PDMS-glycidyl, and (d) bioepoxy/5%POSS-glycidyl. (ii) Transmission electron microscope images of bioepoxy/5%POSS-glycidyl at different areas (a and b).

The tensile and flexural moduli of all resins were found to be equivalent to the moduli of neat bioepoxy.

The impact strength and elongation at break of neat bioepoxy and siloxane modified bioepoxy are shown in Figure 9. The addition of functionalized PDMS-amine showed deterioration in the percent of elongation and the impact strength. This may be due to the fact that the elastomeric PDMS was heterogeneous and immiscible in the bioepoxy matrix, which decreased the interaction between the matrix and the modifier resulting in a decrease in the toughness of the resin. The addition of

PDMS-glycidyl slightly enhanced the elongation at break of the final product.

The incorporation of POSS-glycidyl enhanced the elongation at break and impact strength as presented in Figure 9. The impact strength and elongation at break enhanced by 16 and 29%, respectively, compared to neat epoxy resin. This is due to the presence of nanosized and caged framework of the POSS structure that can absorb impact energy. Moreover, the effect of the epoxy group present in the POSS-glycidyl increased the cross-linking density and produced more anchors in the resin.<sup>32</sup>



**Scheme 2.** Formation of network structure and surface in bioepoxy resin containing PDMS-amine or glycidyl and with POSS-glycidyl. [Color figure can be viewed in the online issue, which is available at [wileyonlinelibrary.com](http://wileyonlinelibrary.com).]



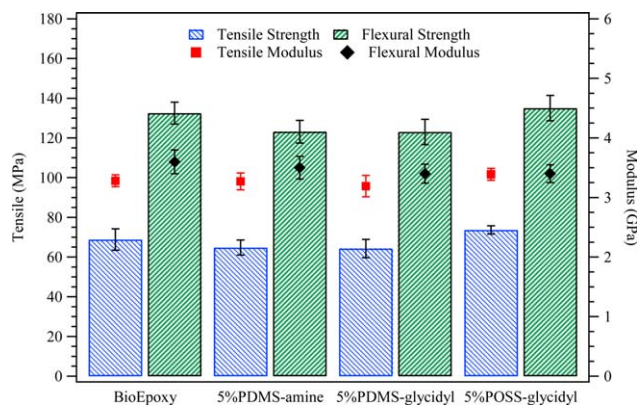


**Figure 8.** Tensile and flexural properties of neat bioepoxy and bioepoxy modified by different siloxanes. [Color figure can be viewed in the online issue, which is available at [wileyonlinelibrary.com](http://wileyonlinelibrary.com).]

### Dynamic Mechanical Analysis

The viscoelastic behaviour of neat bioepoxy resin and bioepoxy modified with different siloxanes are given in Figures 10 and 11. Figure 10 shows that the storage modulus of all bioepoxies with siloxanes is slightly lower than those of neat bioepoxy resin at lower temperature (lower than  $T_g$ ). For example, the storage modulus values of neat bioepoxy, bioepoxy modified with POSS-glycidyl, PDMS-amine and PDMS-glycidyl at 25°C are 3371, 3281, 3054, and 2936 MPa, respectively. At around 95°C (higher than  $T_g$ ), the storage modulus of POSS-glycidyl and PDMS-glycidyl are substantially equivalent to neat bioepoxy. The storage modulus values of neat bioepoxy, bioepoxy modified with POSS-glycidyl, and PDMS-glycidyl at 100°C are 14, 18, and 15 MPa, respectively. The same behavior was observed for epoxy modified with POSS.<sup>45</sup> This indicated that modified bioepoxy with POSS-glycidyl and PDMS-glycidyl has greater dimensional thermal stability than neat bioepoxy.

The  $\tan\delta$ , the glass transition temperature ( $T_g$ ) of neat bioepoxy resin and modified bioepoxy are shown in Figure 11. Neat bioepoxy and modified bioepoxies showed only a single broad  $T_g$ . All modified bioepoxy showed decreased  $T_g$  values compared to neat bioepoxy. For example, the  $T_g$  values of neat bioepoxy and bioepoxy modified with PDMS-amine, PDMS-glycidyl, and

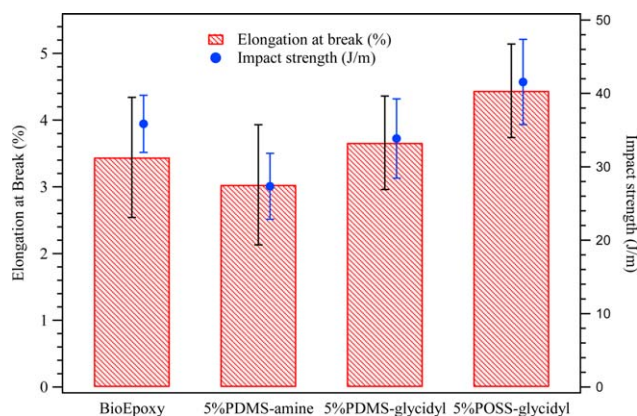


**Figure 9.** Elongation at break and impact strength values of neat bioepoxy and bioepoxy modified by different siloxanes. [Color figure can be viewed in the online issue, which is available at [wileyonlinelibrary.com](http://wileyonlinelibrary.com).]

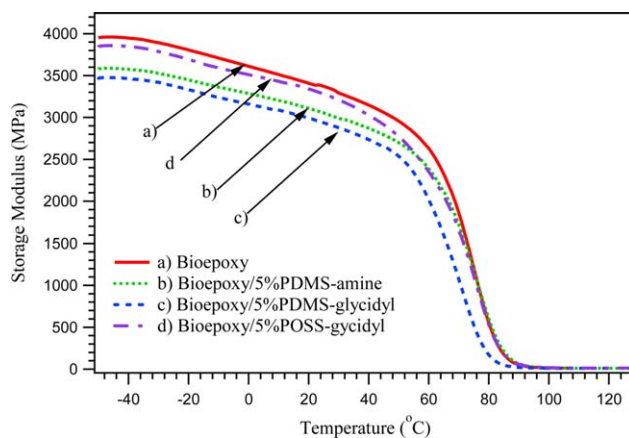


**Figure 10.** Storage modulus values of neat bioepoxy and bioepoxy modified by different siloxanes. [Color figure can be viewed in the online issue, which is available at [wileyonlinelibrary.com](http://wileyonlinelibrary.com).]

POSS-glycidyl are 87, 85, 82, and 84°C, respectively. The decrease in  $T_g$  values compared to neat bioepoxy may be due to plasticization effect of the flexible  $-\text{Si}-\text{O}-\text{Si}-$  linkage.<sup>45</sup>

### Heat Deflection Temperature (HDT) and Coefficient of Linear Thermal Expansion (CLTE)

HDT is the temperature at which a test sample deflects a specific amount under specific load. It represents the upper limit of the dimensional stability of polymers in service. The HDT values for neat bioepoxy and the modified bioepoxies in this study are presented in Figure 12. Neat bioepoxy has HDT value of 61°C. The addition of PDMS terminated with amine or glycidyl did not affect the HDT. However, the addition of POSS-glycidyl has significantly raised the HDT by around 14% compared to neat bioepoxy. Tucker *et al.*<sup>40</sup> observed an increase in the HDT when blending epoxy resin with POSS. The author clarified the improvement in the HDT resulted from POSS, which works as a crosslinking hub and restricts the chain mobility of the epoxy matrices. POSS-glycidyl has outstanding heat resistant resulting from the caged structure and nano size of POSS as confirmed

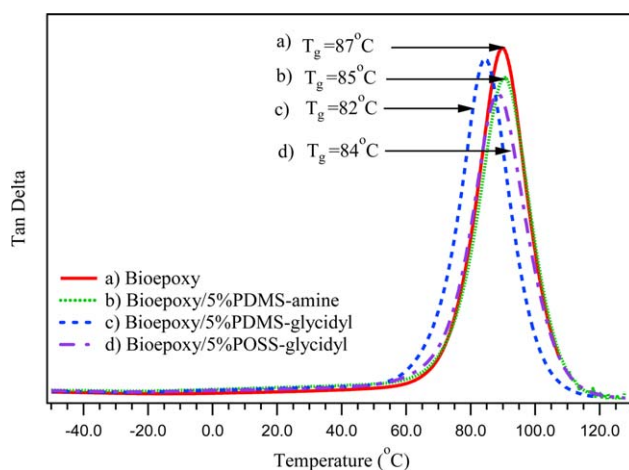


**Figure 11.**  $\tan\delta$  values of neat bioepoxy and bioepoxy modified by different siloxanes. [Color figure can be viewed in the online issue, which is available at [wileyonlinelibrary.com](http://wileyonlinelibrary.com).]

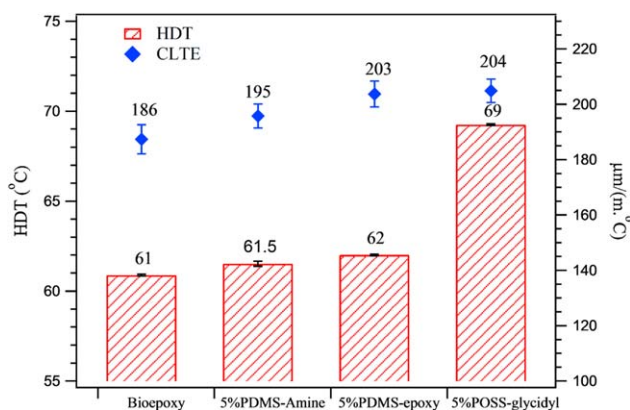


**Figure 12.** Heat deflection temperature and coefficient of linear thermal expansion values of neat bioepoxy and bioepoxy modified by different siloxanes. [Color figure can be viewed in the online issue, which is available at [wileyonlinelibrary.com](http://wileyonlinelibrary.com).]

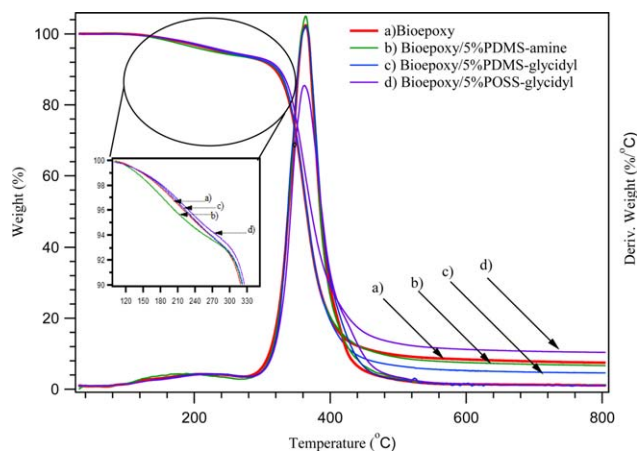
from TEM.<sup>28</sup> Therefore, the incorporation of POSS-glycidyl to neat bioepoxy provides high HDT values which is useful for fabricating high temperature resistant composites compared to neat bioepoxy.

Figure 12 represents the effect of different types of siloxanes on the coefficient of linear thermal expansion (CLTE). The CLTE for modified bioepoxy blends increased with different types of siloxanes compared to neat bioepoxy. This behavior is due to the higher thermal expansion of the filler compared to neat bioepoxy. However, the CLTE values of bioepoxy modified with POSS-glycidyl showed higher value than terminated PDMS due to the constraint from the hard POSS like clay or layered silicates.<sup>34</sup>

### Thermal Properties

The effect of siloxane additives on the thermal stability of the neat bioepoxy resins was examined using TGA. Figure 13 displays the TGA and derivative TGA graphs of neat bioepoxy and modified bioepoxy blends. The degradation temperatures at 5 wt % ( $T_5$ ) and the residue at 800°C are presented in Table II.

Bioepoxy resin is an aliphatic molecule containing epoxidized pine oil and provides lower thermal stability. The introduction of 5%PDMS-amine into neat bioepoxy decreased the thermal stability and reduced the degradation temperature as shown in Table II. This could be because the residual amine hardener did not react with PDMS-amine and decomposed at lower temperatures. In contrast, the introduction of 5%PDMS-glycidyl did not show any effect on the thermal properties. However, the



**Figure 13.** TGA and DTG curves of neat bioepoxy and bioepoxy modified by different siloxanes. [Color figure can be viewed in the online issue, which is available at [wileyonlinelibrary.com](http://wileyonlinelibrary.com).]

addition of 5%POSS-glycidyl improved the thermal stability of the bioresins.  $T_5$  improved 9°C by the addition of 5% POSS-glycidyl to the bioresins. This could be due to presence of the nanosized POSS network which has a high heat resistance property.<sup>32</sup>

To calculate the thermal stability of the bioresins, the static heat-resistant index ( $T_s$ ) was used.<sup>46,47</sup> It is calculated from  $T_5$  and  $T_{30}$  weight loss of the bioresins. From Table II, the  $T_s$  values of the bioresins were equivalent to the behavior of the thermal degradation of all bioresins. These results indicated that the bioepoxy modified with PDMS-glycidyl possessed a higher thermal stability compared to neat bioepoxy. In contrast, PDMS-amine possessed a lower thermal stability compared to neat bioepoxy. Neat epoxy modified with 5%POSS-glycidyl showed a higher char yield value compared to other bioresins indicating that there is an improved flame retardance.<sup>48</sup> This is due to presence of POSS-glycidyl which restricts the thermal motion and retards the organic decompositions.

The values of  $T_g$  of neat bioepoxy and modified bioepoxy are presented in Figure 14. All siliconized bioepoxies exhibit a single  $T_g$ , which indicates the existence of intercrosslinking structure. The  $T_g$  values of all modified bioepoxies are decreased compared to neat bioepoxy. Li *et al.*<sup>45</sup> reported that the addition of polyphenylsilsequioxane to epoxy resin decreased the  $T_g$  of material. This is due to decreasing in the crosslinking density. Here, the decreased  $T_g$ s resulted from the plasticization of siloxane on bioepoxy matrix.

**Table II.** TGA of Neat Bioepoxy and Siloxane Modified Bioepoxy<sup>a</sup>

Code	$T_5$ (°C)	$R_{800}$ (%)	$T_s$	Density (g/cm <sup>3</sup> )
Bioepoxy	242	7.5	151	1.142 ± 0.001
Bioepoxy/5%PDMS-amine	228	6.2	148	1.133 ± 0.001
Bioepoxy-5%PDMS-glycidyl	244	4.6	151	1.136 ± 0.001
Bioepoxy-5%POSS-glycidyl	251	10.38	154	1.152 ± 0.004

<sup>a</sup>  $T_5$ ,  $T_s$ : are the decomposition temperatures at 5% and the static heat-resistant index, respectively.  $R_{800}$  is the char yield at 800°C.

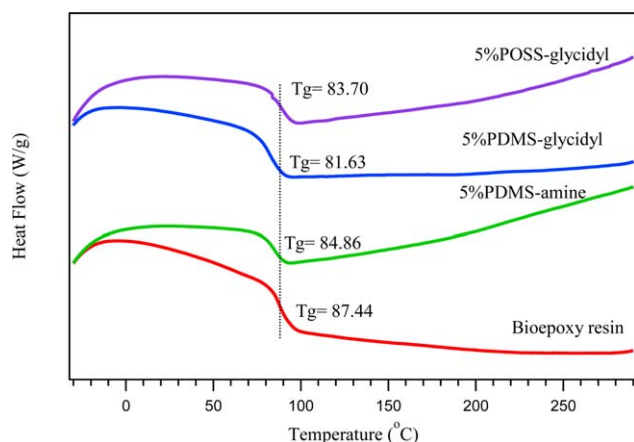


**Figure 14.** DSC curves of neat bioepoxy and bioepoxy modified by different siloxanes. [Color figure can be viewed in the online issue, which is available at [wileyonlinelibrary.com](http://wileyonlinelibrary.com).]

### Density

The density of neat bioepoxy and siloxane modified bioepoxy are presented in Table II. Neat bioepoxy has a density of 1.14 g/cm<sup>3</sup>, which is lower than commercial epoxy resin 1.18–1.35 g/cm<sup>3</sup>.<sup>34,49</sup> The bioepoxy modified with PDMS-amine or glycidyl had a density lower than neat bioepoxy of approximately 1.136 g/cm<sup>3</sup> due to low molecular weight of the modifier. However, with the incorporation of POSS-glycidyl, the density of the bioresin increased slightly to a value of 1.15 g/cm<sup>3</sup>. This result was in agreement with the previous study of POSS/epoxy system.<sup>34</sup>

### CONCLUSIONS

A new hybrid system based on bioepoxy resins and 5 wt % functionalized siloxane was successfully prepared and examined through morphological and thermomechanical analysis. The cure kinetics of all bioepoxy systems was investigated using Kissinger and Flynn–Wall–Ozawa equations and found that the activation energy ( $E_a$ ) exhibits a higher value compared to neat bioepoxy. SEM and TEM images indicated that the incorporation of POSS-glycidyl displayed a good miscibility between the matrix and the modifier, homogeneous at the nanoscale. The incorporation of PDMS-amine or PDMS-glycidyl was shown to have no drastic effect on the tensile and flexural properties of the bioresins, but could lead to a deterioration in the impact strength compared to neat bioepoxy. However, the inclusion of POSS-glycidyl enhanced the impact strength and percent of elongation of the bioresins. DMA analysis revealed that the functionalized siloxane decreased the storage modulus of the bioresins. The thermal properties, such as decomposition temperature, HDT, and CLTE were improved by inclusion of POSS-glycidyl. Finally, through the analysis of the morphological and mechanical properties, the bioepoxy with 5% POSS-glycidyl had the best properties compared to other fillers and can be a good candidate for enhancement the properties of epoxy resin.

The authors would like to thank the Ontario Ministry of Agriculture, Food, and the Rural Affairs (OMAFRA) New Directions

Research Program; OMAFRA/University of Guelph-Bioeconomy for Industrial Uses Research Program; Natural Sciences and Engineering Research Council of Canada (NSERC) Canada, Collaborative Research and Development (CRD) Grant Program; Grain Farmers of Ontario (GFO); and Ontario Ministry of Research and Innovation (MRI) for their financial support to carry out this research work.

### REFERENCES

- Auvergne, R.; Caillol, S.; David, G.; Boutevin, B.; Pascault, J.-P. *Chem. Rev.* **2014**, *114*, 1082.
- Thomas, R.; Durix, S.; Sinturel, C.; Omonov, T.; Goossens, S.; Groeninckx, G.; Moldenaers, P.; Thomas, S. *Polymer* **2007**, *48*, 1695.
- Kawaguchi, T.; Pearson, R. A. *Polymer* **2003**, *44*, 4239.
- Ruiz-Perez, L.; Royston, G. J.; Fairclough, J. P. A.; Ryan, A. J. *Polymer* **2008**, *49*, 4475.
- Pearson, R. A.; Yee, A. F. *Polymer* **1993**, *34*, 3658.
- Yahyaie, H.; Ebrahimi, M.; Tahami, H. V.; Mafi, E. R. *Prog. Org. Coat.* **2013**, *76*, 286.
- Ratna, D.; Banthia, A. K. *Macromol. Res.* **2004**, *12*, 11.
- Miyagawa, H.; Mohanty, A. K.; Misra, M.; Drzal, L. T. *Macromol. Mater. Eng.* **2004**, *289*, 629.
- Miyagawa, H.; Misra, M.; Drzal, L. T.; Mohanty, A. K. *Polym. Eng. Sci.* **2005**, *45*, 487.
- Gupta, A. P.; Ahmad, S.; Dev, A. *Polym. Eng. Sci.* **2011**, *51*, 1087.
- Fombuena, V.; Sánchez-Nácher, L.; Samper, M. D.; Juárez, D.; Balart, R. *J. Am. Oil Chem. Soc.* **2013**, *90*, 449.
- Stemmelen, M.; Pessel, F.; Lapinte, V.; Caillol, S.; Habas, J. P.; Robin, J. J. *J. Polym. Sci. A Polym. Chem.* **2011**, *49*, 2434.
- Tan, S. G.; Chow, W. S. *Polym. Plast. Technol. Eng.* **2010**, *49*, 1581.
- Eissen, M.; Metzger, J. O.; Schmidt, E.; Schneidewind, U. *Angew. Chem. Int. Ed.* **2002**, *41*, 414.
- Li, F.; Larock, R. C. *J. Appl. Polym. Sci.* **2001**, *80*, 658.
- Ratna, D. *Polym. Int.* **2001**, *50*, 179.
- Pupure, L.; Doroudgarian, N.; Joffe, R. *Polym. Compos.* **2014**, *35*, 1150.
- Raquez, J. M.; Deléglise, M.; Lacrampe, M. F.; Krawczak, P. *Prog. Polym. Sci.* **2010**, *35*, 487.
- Rey, L.; Poisson, N.; Maazouz, A.; Sautereau, H. *J. Mater. Sci.* **1999**, *34*, 1775.
- Ananda Kumar, S.; Sankara Narayanan, T. S. N. *Prog. Org. Coat.* **2002**, *45*, 323.
- Fan, W.; Wang, L.; Zheng, S. *Macromolecules* **2008**, *42*, 327.
- Gong, W.; Zeng, K.; Wang, L.; Zheng, S. *Polymer* **2008**, *49*, 3318.
- Guo, Q.; Chen, F.; Wang, K.; Chen, L. *J. Polym. Sci. B: Polym. Phys.* **2006**, *44*, 3042.
- Xu, Z.; Zheng, S. *Polymer* **2007**, *48*, 6134.



25. Murugavel, R.; Voigt, A.; Walawalkar, M. G.; Roesky, H. W. *Chem. Rev.* **1996**, *96*, 2205.
26. Kannan, R. Y.; Salacinski, H. J.; Butler, P. E.; Seifalian, A. M. *Acc. Chem. Res.* **2005**, *38*, 879.
27. Sanchez, C.; Soler-Illia, G. J. d. A. A.; Ribot, F.; Lalot, T.; Mayer, C. R.; Cabuil, V. *Chem. Mater.* **2001**, *13*, 3061.
28. Matějka, L.; Strachota, A.; Pleštil, J.; Whelan, P.; Steinhart, M.; Šlouf, M. *Macromolecules* **2004**, *37*, 9449.
29. Choi, J.; Yee, A. F.; Laine, R. M. *Macromolecules* **2003**, *36*, 5666.
30. Zucchi, I. A.; Galante, M. J.; Williams, R. J. J.; Franchini, E.; Galy, J.; Gérard, J.-F. *Macromolecules* **2007**, *40*, 1274.
31. Iyer, S.; Schiraldi, D. A. *Macromolecules* **2007**, *40*, 4942.
32. Ni, C.; Ni, G.; Zhang, L.; Mi, J.; Yao, B.; Zhu, C. *J. Colloid Interface Sci.* **2011**, *362*, 94.
33. Kim, G. M.; Qin, H.; Fang, X.; Sun, F. C.; Mather, P. T. *J. Polym. Sci. B: Polym. Phys.* **2003**, *41*, 3299.
34. Li, Q.; Hutcheson, S. A.; McKenna, G. B.; Simon, S. L. *J. Polym. Sci. B: Polym. Phys.* **2008**, *46*, 2719.
35. Wen, X.; Wang, X.; Cai, Z.-Q.; Pi, P.; Cheng, J.; Yang, Z. *High Perform. Polym.* **2011**, *23*, 477.
36. Kissinger, H. E. *Anal. Chem.* **1957**, *29*, 1702.
37. Ozawa, T. *J. Therm. Anal.* **1970**, *2*, 301.
38. Barral, L.; Cano, J.; López, J.; López-Bueno, I.; Nogueira, P.; Abad, M. J.; Ramírez, C. *J. Polym. Sci. B: Polym. Phys.* **2000**, *38*, 351.
39. Velan, T. V.; Bilal, I. M. *Bull. Mater. Sci.* **2000**, *23*, 425.
40. Tucker, S. J.; Fu, B.; Kar, S.; Heinz, S.; Wiggins, J. S. *Compos. A: Appl. Sci. Manufact.* **2010**, *41*, 1441.
41. Ni, C.; Ni, G.; Zhang, S.; Liu, X.; Chen, M.; Liu, L. *Colloid Polym. Sci.* **2010**, *288*, 469.
42. Strachota, A.; Whelan, P.; Kříž, J.; Brus, J.; Urbanová, M.; Šlouf, M.; Matějka, L. *Polymer* **2007**, *48*, 3041.
43. Sobhani, S.; Jannesari, A.; Bastani, S. *J. Appl. Polym. Sci.* **2012**, *123*, 162.
44. Lin, L.-L.; Ho, T.-H.; Wang, C.-S. *Polymer* **1997**, *38*, 1997.
45. Li, G. Z.; Wang, L.; Toghiani, H.; Daulton, T. L.; Koyama, K.; Pittman, C. U. *Macromolecules* **2001**, *34*, 8686.
46. Aouf, C.; Nouaillhas, H.; Fache, M.; Caillol, S.; Boutevin, B.; Fulcrand, H. *Eur. Polym. J.* **2013**, *49*, 1185.
47. Chiu, Y.-C.; Chou, I. C.; Tseng, W.-C.; Ma, C.-C. M. *Polym. Degrad. Stabil.* **2008**, *93*, 668.
48. Selvi, M.; Devaraju, S.; Vengatesan, M. R.; Go, J. S.; Kumar, M.; Alagar, M. *RSC Adv.* **2014**, *4*, 8238.
49. Cho, H.; Liang, K.; Chatterjee, S.; Pittman, C. U., Jr. *J. Inorg. Organomet. Polym. Mater.* **2005**, *15*, 541.